THE JOURNAL OF BIOLOGICAL CHEMISTRY VOL. 288, NO. 12, pp. 8136–8145, March 22, 2013

H_2O_2 Regulates Lung Epithelial Sodium Channel (ENaC) via Ubiquitin-like Protein Nedd8

Received for publication, November 8, 2012, and in revised form, January 24, 2013 Published, JBC Papers in Press, January 28, 2013, DOI 10.1074/jbc.M112.389536

Charles A. Downs[‡§], **Amrita Kumar**[§], **Lisa H. Kreiner**[§¶], **Nicholle M. Johnson**[§¶], **and My N. Helms**[§¶1]

From the [‡]*Nell Hodgson Woodruff School of Nursing,* [¶]*Department of Pediatrics Center for Developmental Lung Biology, and the* [§]*Department of Physiology, Emory University School of Medicine, Atlanta, Georgia 30322*

Background: Proteolytic degradation of epithelial sodium channels (ENaC) assists in regulating net salt and water balance in lung epithelia.
Results: H_2O_2 increases surface expression of α-ENaC, transepithelial Na transport, and alveolar fluid clearance via redox-sensitive Nedd8.
Conclusion: Redox-sensitive Nedd8 is involved in the ubiquitination of lung ENaC.
Significance: Understanding ROS-mediated signaling of lung ENaC is crucial for understanding pulmonary physiology and pathology.

Redundancies in both the ubiquitin and epithelial sodium transport pathways allude to their importance of proteolytic degradation and ion transport in maintaining normal cell function. The classical pathway implicated in ubiquitination of the epithelial sodium channel (ENaC) involves Nedd4-2 regulation of sodium channel subunit expression and has been studied extensively studied. However, less attention has been given to the role of the ubiquitin-like protein Nedd8. Here we show that Nedd8 plays an important role in the ubiquitination of ENaC in alveolar epithelial cells. We report that the Nedd8 pathway is redox-sensitive and that under oxidizing conditions Nedd8 conjugation to Cullin-1 is attenuated, resulting in greater surface expression of α-ENaC. This observation was confirmed in our electrophysiology studies in which we inhibited Nedd8-activating enzyme using MLN4924 (a specific Nedd8-activating enzyme inhibitor) and observed a marked increase in ENaC activity (measured as the product of the number of channels (N) and the open probability (Po) of a channel). These results suggest that ubiquitination of lung ENaC is redox-sensitive and may have significant implications for our understanding of the role of ENaC in pulmonary conditions where oxidative stress occurs, such as pulmonary edema and acute lung injury.

Epithelial sodium channels (ENaC)[2] play a key role in maintaining salt and water balance in the body. Three homologous ENaC subunits (α, β, and γ) are primarily expressed in the kidney, colon, and lung in a fixed stoichiometry. The α-ENaC subunit has been described as the most abundant subunit expressed at the cell membrane (1) capable of forming non-selective amiloride-sensitive current alone, or alongside β- and γ-ENaC subunits (2) to transport Na with high specificity. Mice that lack expression of α-ENaC fail to thrive because of an inability to clear lung fluid, which highlights the importance of studying lung ENaC (3). Additionally, ENaC has a relatively short half-life (estimated $t_{1/2}$ between 1–4 h) (4, 5), and as such, studying the regulatory factors that influence insertion or removal of Na channel subunits in the apical membrane may be key in advancing understanding of salt-wasting and hyperabsorptive conditions. Indeed, changes in proteolysis and/or inappropriate activation of sodium channels at the membrane have been implicated as the underlying cause of pseudohyperaldosteronism type 1, Liddle's syndrome, and cystic fibrosis lung disorders (6–8). Comprehending the role of Nedd8 (an ubiquitin-like protein) and its associated E3-ligases in Na transport could lead to improved therapies for both hypo- and hyperabsorptive diseases.

Ubiquitin controls the cellular levels of proteins. Like all proteins labeled for degradation, polyubiquitination of ENaC requires a series of enzymes that act in sequence. Generally speaking, ubiquitin is first charged by E1, an ubiquitin activation enzyme, and then transferred to an ubiquitin carrier protein, E2, followed by the addition of ubiquitin to target proteins via an ubiquitin ligase (E3). HECT domain E3 enzymes, such as Nedd4-2, form high-energy thioester bonds between ubiquitin and the E3 ligase before its transfer to, for example, the ENaC substrate, where it is tagged for proteolytic degradation. Alternatively, protein degradation can occur via proteolytic elimination via ubiquitin-like modifiers, albeit via distinct mechanisms. Currently, several ubiquitin-like modifiers, such as Nedd8, have been identified.

Nedd8 shares 80% homology with ubiquitin (9). Again, similar to the ubiquitin proteolytic pathway, Nedd8 requires the coordinated action of APP-BP1 (a heterodimeric E1-like enzyme) and Ubc12 (an E2-like enzyme) (Fig. 1). Unlike ubiquitination, however, neddylation of Cullin-1 is required for the Cullin-1·RING·E3 complex to form to transfer ubiquitin from its E2 enzyme (Ubc12) to the target (whereas ubiquitination transfers ubiquitin from E2 → E3 → directly to → target). Cullin-1, Skp1, Rbx, and an F-box protein comprise the E3 complex required for complete neddylation of substrate protein. Addi-

[1] To whom correspondence should be addressed: Department of Pediatrics, Center for Developmental Lung Biology, School of Medicine, Emory University, 2015 Uppergate Dr. NE, 316-K, Atlanta, GA 30322. Tel.: 404-727-8571; Fax: 404-727-3236; E-mail: mhelms@emory.edu.
[2] The abbreviations used are: ENaC, epithelial sodium channel(s), T1 cell, type 1 cell; T2 cell, type 2 cell; HSC, highly selective cation; NSC, non-selective cation; ROS, reactive oxygen species.

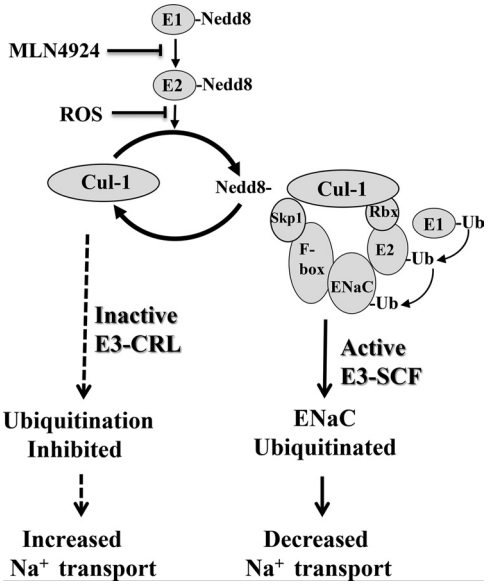

FIGURE 1. **Model for redox regulation of ENaC where reactive ROS or MLN4924 inactivates the Ubc12 enzyme, hindering E3-CRL complex formation (*i.e.* ubiquitination of the target substrate).** In this model, oxidizing conditions (or MLN4924 inhibition of neddylation) attenuates ubiquitination of α-ENaC (*dashed arrows*). Conversely, neddylation (Cul-1-Nedd8 conjugation) results in ubiquitination of α-ENaC (*solid arrow*). Skp1, Cul-1, and F-box comprise the E3 ligase (*E3-SCF*) alongside Rbx, a small zinc-binding domain. This is called the RING finger, to which the E2-ubiquitin conjugate binds. *Cul-1*, Cullin-1; *Ub*, ubiquitin.

tionally, neddylation differs mechanistically from ubiquitination in that Nedd8 conjugation to Ubc12 at Cys-111 is redox-sensitive (10). Under oxidizing conditions, Ubc12-Cys-111 cannot be charged with Nedd8. As such, Cullin-1 remains inactive, leading to a reduction in target protein (*e.g.* ENaC) degradation. This is a fascinating mechanism by which ubiquitin-like modifiers can impart redox sensitivity to a targeted protein (see proposed model in Fig. 1).

Because we have shown that reactive oxygen species play an important role in up-regulation of ENaC activity in the lung (11), we tested the hypothesis that Nedd8 and its associated E2 carrier protein (Ubc12) and E3-SCF ligase play a key role in regulating the expression and activity of ENaC in alveolar type 1 (T1) cells and alveolar type 2 (T2) cells.

MATERIALS AND METHODS

Animal Care—All procedures conformed to the National Institutes of Health animal care and use guidelines and were approved by the Institutional Animal Care and Use Committee of Emory University. Twelve-week-old female C57Bl/6 mice were purchased from The Jackson Laboratory (Bar Harbor, ME). 8- to 12-week-old male Sprague-Dawley rats were purchased from Charles River Laboratories, Inc. (Wilmington, MA).

Chemicals and Reagents—Unless stated otherwise, all chemicals and reagents were purchased from Sigma-Aldrich (St. Louis, MO).

Isolation of Primary Alveolar Type 2 (T2) cells—Rat lungs were perfused via the pulmonary artery with 50 ml of solution A (5.5 mM dextrose, 10 mM HEPES, 2 mM $CaCl_2$, 1.3 mM $MgSO_4$, 140 mM NaCl, and 5 mM KCl (pH 7.4)) followed by washing with solution B (5.5 mM dextrose, 10 mM HEPES, 197 mM EGTA, 140 mM NaCl, 5 mM KCl). Lungs were excised, lavaged tracheally with 13 mg of elastase reconstituted in 40 ml of solution A for 30 min at 37°C, and then minced in solution A supplemented with 2 mg/ml of DNase I and 50% FBS. Pneumocytes were successively filtered through 100-μm and 40-μm filters, centrifuged, and resuspended in selection media consisting of DMEM/F12 50/50, 2 mM L-glutamine, and 20 units/ml of penicillin-streptomycin. The cell suspension was then panned for 1 h at 37 °C on an IgG-coated Petri dish. Non-adherent T2 cells were removed and centrifuged at 1200 × *g* for 5 min in DMEM-F-12 culture medium (supplemented with 10% FBS, 2 mM L-glutamine, 20 units/ml of penicillin-streptomycin, 84 μM gentamycin, 1 μM dexamethasone). Using this protocol we obtained primary T2 cells with > 95% purity.

Lung Slice Preparation—Rat lung slice preparation was performed as described previously (11). Lung slices were maintained in 50:50 ice-cold DMEM/F-12 culture medium (supplemented with10% FBS, 2 mM L-glutamine, 1 μM dexamethasone, 84 μM gentamicin, and 20 units/ml penicillin-streptomycin). Alveolar T1 cells were patched for single channel analysis within 6 h of tissue preparation.

Patch Clamp Analysis—Single channel patch clamp analysis of T1 and T2 cells was performed in the cell-attached configuration. Micropipettes were pulled from borosilicate glass capillaries (TW-150, World Precision Instruments), and Gigaohm seals were formed between the electrode tip and the cell membrane following gentle negative pressure. Electrode and saline solution contain 96 mM NaCl, 3.4 mM KCl, 0.8 mM $CaCl_2$, 0.8 mM $MgCl_2$, and 10 mM HEPES, with pH adjusted to 7.4 with NaOH. Following a control recording period, H_2O_2 or MLN4924 (Millenium Pharmaceuticals) was applied to the same cell-attached recording. Channel activity (NPo, the product of the number of channels and the open probability) was calculated from pClampfit 9.2 data software (Molecular Devices). Highly selective cation (HSC) channel and non-selective cation (NSC) channel conductances were calculated following H_2O_2 and MLN4924 treatment using a minimum of three holding potentials.

Protein Biochemistry—T2 cells were resuspended in cell culture medium and treated in suspension with H_2O_2 (0.1–1.0 mM) or the specific Nedd8-activating enzyme inhibitor MLN4924 (0.1–10 nM) at 37 °C and 5% CO_2 for 5, 15, 30, 60, or 120 min (12). After treatment, cells were washed with ice-cold PBS supplemented with 1× protease inhibitors (Calbiochem) and pelleted. Standard immunoblotting techniques were used. Lysates were electrophoresed on a 10% acrylamide gel, transferred to a nitrocellulose membrane (Bio-Rad), and then immunoblotted with anti-α ENaC C-20 antibody directed against the C-terminal domain (Santa Cruz Biotechnology, Inc.). For immunoprecipitation assays, cells were lysed in EBC buffer (50 mM Tris (pH 8.0), 120 mM NaCl, and 0.5% Nonidet P-40 supplemented with protease inhibitor mixture (Calbiochem) and phosphatase inhibitors 1 and 11 (Calbiochem)). Thereafter, 800 mg of lysate was incubated with either (1–2 mg) α-ENaC, Cullin-1, Nedd8, Ubc12, or IgG-coated beads overnight, followed by 1-h room-temperature incubation with protein G-Sepharose beads (Pierce). Immunocomplexes were washed five times

with NETN buffer (20 mM Tris (pH 8.0), 100 mM NaCl, 1 mM EDTA, and 0.5% Nonidet P-40) before SDS-PAGE analysis (± DTT) and immunoblotted with antibodies of interest (as indicated in the figure legends). To detect immunoreactive signal on Western blot analyses, IgG-HRP-labeled secondary antibody (KPL, Gaithersburg, MD) was added at a concentration of 1 mg/10 ml in EBC buffer and incubated for 1 h at room temperature. An alkaline phosphatase signal was detected using CDP-Star chemiluminescent substrate for AP (Tropix, Bedford, MA). Blots were analyzed on a Carestream imaging station GL4000 (New Haven, CT) and compatible Carestream Molecular imaging software.

Biotinylation of Apical Membrane Proteins—After treatment with either H_2O_2 or MLN4924, T2 cells were washed with ice-cold PBS, and apical membrane proteins were biotinylated with 0.5 mg/ml of S-S biotin (Pierce) in borate buffer containing 85 mM NaCl, 4 mM KCl, 15 mM $Na_2B_4O_7$ (pH 8.0)) for 30 min. Cells were then washed three times in ice-cold PBS, and biotinylation was quenched with DMEM supplemented with 10% horse serum and 125 mM lysine. Supernatant protein concentrations were determined using a standard Bradford assay. Neutravidin beads (Pierce) were combined with 300 mg of biotinylated protein and incubated overnight at 4 °C. Streptavidin-bound protein was collected in 1× SDS sample buffer, heated to 95 °C for 3 min, and then separated by SDS-PAGE.

Cycloheximide Chase—Primary rat alveolar T2 cells were treated in a 0.01% solution of cycloheximide (Sigma) with or without 10 nM MLN4924. Protein was harvested at 0, 5, 15, 30, 60, and 120 min, immunoblotted for α-ENaC, and then protein expression normalized to β-actin.

Real-time PCR—Total RNA was extracted from rat T2 cells using an RNeasy isolation kit (Qiagen) following the protocol of the manufacturer. RNA was then treated with DNaseI and reverse-transcribed using Superscript II RNaseH-reverse transcriptase (Invitrogen). The level of ENaC subunit mRNA expression was determined using the following pairs of forward and reverse primers: α-ENaC, TGC TCC TGT CAC TTC AGC AC (forward) and CCC CTT GCT TAG CCT GTT C (reverse); β-ENaC, CCC CTG ATC GCA TAA TCC TA (forward) and GCC CCA GTT GAA GAT GTA GC (reverse); and γ-ENaC, ACC CTT TCA TCG AAG ACG TG (forward) and CCT CTG TGC ACT GGC TGT AA (reverse). Threshold levels of mRNA expression (ΔΔCt) were normalized to mouse GAPDH levels, and values represent the mean of triplicate samples ± S.E. Data are representative of three independent studies.

Fluoroscopic Determination of Lung Fluid Clearance—Animals were tracheally instilled with a saline challenge of 5μL/g body weight, as described in Refs. 11, 13. The saline solution contained 96 NaCl, 3.4 KCl, 0.8 $CaCl_2$, 0.8 $MgCl_2$, and 10 HEPES, with the pH adjusted to 7.4 with NaOH. Immediately following instillation (I_o), animals were radiographed using an *in vivo* MS FX Pro small animal imager (Carestream Health) with an E-Z Anesthesia unit (Palmer, PA) attached to deliver oxygen and 2% isoflurane. Animals were X-rayed at 5-min intervals (with 2-min exposure times) up to 120 min with the following acquisition settings: 2X2 binning, 180-mm field of view, and 149-μA x-ray current. X-ray density was quantified using Carestream Health MI software with a defined 5-mm^2 region of interest. All fluoroscopic regions of interest (ROI) were background-corrected and normalized to the initial x-ray intensity (I_o) to make comparisons between time points and experimental groups. Changes in lung fluid volume are expressed as $I\text{-}I_o$, where I is the x-ray density at a respective time point and I_o is the initial x-ray density following the saline challenge.

Statistical Evaluation—All data are summarized as mean ± S.E. Single comparisons were performed using paired Student's *t* tests. Multiple comparisons were performed using one-way analysis of variance followed by the Bonferroni post-hoc test for pair-wise comparisons. *p* values of ≤ 0.05 were considered statistically significant.

RESULTS

Lung ENaC Is Redox-sensitive—To show that lung ENaC activity is redox-sensitive, we treated alveolar T2 cells with 250 μM H_2O_2 while maintaining a Gigaohm seal in the cell-attached configuration. Fig. 2, *A–C*, shows a representative trace demonstrating an increase in ENaC NPo following ≥ 35 min of H_2O_2 application to the extracellular bath (Fig. 2*D*, $n = 4$). A comparison of ENaC activity from all cells observed show that HSC channel ($\gamma = 6$ pS ± 1.1 S.E. from mean) and NSC channel ($\gamma = 11 \pm 0.8$ pS) channels are activated following H_2O_2 stimulation of T2 cells (Fig. 2, *E–F*, $n = 4$).

Prior to using a commercially available anti-α-ENaC C-20 antibody directed against the C-terminal epitope, we characterized the binding specificity of this antibody under reducing (*+DTT*) and non-reducing (*-DTT*) conditions. As shown in Fig. 3*A*, the predominate immunoreactive band detected using this antibody is ~65 kDa, although a larger 150 kDa band can be faintly detected under non-reducing conditions (discussed below). In Fig. 3*B*, alveolar T2 cells treated with 250 μM H_2O_2 (applied to the culture media) showed that protein expression of α-ENaC significantly increases following oxidation. The graph in Fig. 3*B* quantifies the robust increase in the 65 kDa cleaved form of α-ENaC (14, 15) from three independent observations. Interestingly, a second immunoreactive band of ~150 kDa in molecular size was also robustly detected using the anti-α-ENaC C-20 antibody following H_20_2 exposure (as indicated by the *asterisk* in Fig. 3*B*). Although the molecular identity of this larger band remains unknown, peptide competition indicates antibody specificity (Fig. 3*A*, *right panel*). Fig. 3*B* shows that H_2O_2 significantly increased total α-ENaC at 60 and 120 min ($n = 3$, * = $p < 0.05$). In Fig. 3*C*, we show that surface expression (biotinylated) of ENaC was enhanced significantly following 60- and 120-min exposure to H_2O_2 (* = $p < 0.05$). Interestingly, only the cleaved form of α-ENaC was biotinylated (65 kDa) before and after H_2O_2 exposure (and the larger 150-kDa immunoreactive band detected using whole cell lysate was not observed in Fig. 3*C*). Additionally, β-tubulin labeling of biotinylated protein indicates that intracellular protein did not pull down. Positive β-tubulin signal control (from cell lysate) is also included in Fig. 3*C*.

Real-time PCR evaluation of α, β, and γ ENaC mRNA levels following H_2O_2 treatment of T2 cells indicates no change in transcription of the sodium channel subunits (Fig. 3*D*). Together, these data indicate that H_2O_2 treatment enhances

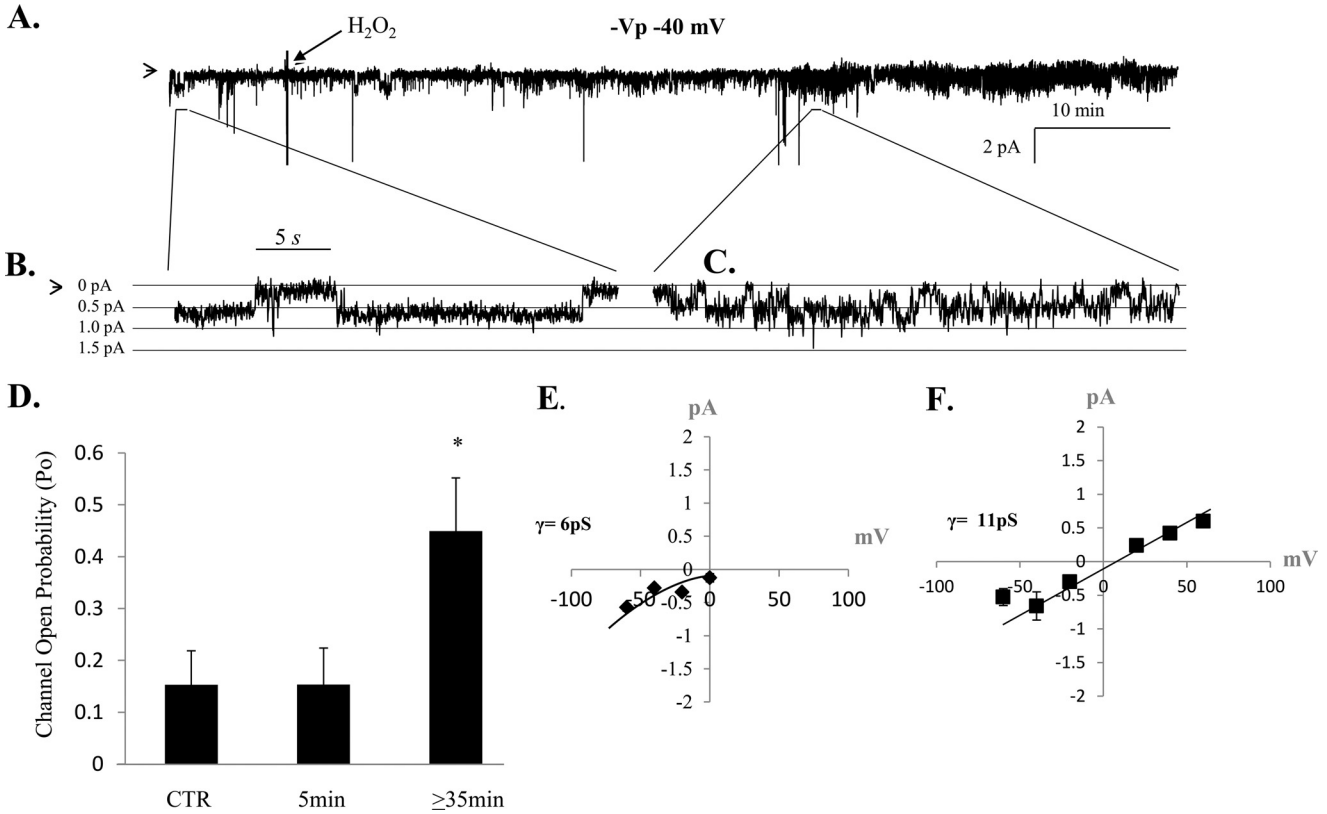

FIGURE 2. **Lung ENaC is redox-sensitive.** *A*, continual, representative, single channel patch clamp recording obtained from isolated primary alveolar T2 cell before and after 250 μM H_20_2 application (as indicated on the trace). *B* and *C*, higher resolution of the single channel recording shown in *A*, 30 s in duration, showing increases in open probability (*Po*), the fraction of time a channel is open, following H_20_2 treatment. In *A–C*, the *arrow* denotes the closed state, and *downward deflections* from the closed state represent inward Na current. *D*, average Po values from four independent observations show that ENaC activity significantly increases following H_20_2 treatment. Data were sampled from 5-min recording periods before, 5–10 min after, and beyond 30 min of hydrogen peroxide application. *, $p < 0.05$. *E* and *F*, chord conductances (γ) were calculated following H_20_2 treatment, showing HSC (Ave $\gamma = 6 \pm 1.1$ pS) and NSC (Ave $\gamma = 11 \pm 0.85$ pS) channel activity under oxidizing conditions.

sodium channel activity, possibly by increasing the resident time of channels in the plasma membrane. Below, we explore the possibility that redox-sensitive proteolytic pathways play an important role in regulating sodium channel activity (NPo) under oxidizing conditions.

MLN4924 Increases Surface ENaC Activity—MLN4924 (IC_{50} 4.7 nM) is a specific inhibitor of Nedd8-(E1)-activating enzyme (12). As such, this compound has been shown to be effective in controlling the activity of the Cullin-RING subtype of ubiquitin ligases, thereby regulating the turnover of proteins in the plasma membrane (12). In Fig. 4*A*, we show that activated Cullin, Cullin-1 conjugated with Nedd8, is ~95 kDa (in the presence of DTT). In Fig. 4*B*, we show that T2 cells are indeed responsive to 10 and 100 nM MLN4924 treatment, as detection of Cullin-Nedd8 conjugation decreases following MLN4924 inhibition of the E1 enzyme without changes in β-actin protein levels. Cullin-Nedd8 conjugates decreased significantly with MLN4924 treatment (compared with time-matched controls, * = $p < 0.05$). Fig. 4, *C* and *D*, shows that MLN4924 disruption of Cullin-Nedd8 conjugation leads to increases in total (*C*) and biotinylated (*D*) α-ENaC protein (* = $p < 0.05$). The 65-kDa immunoreactive band is shown and quantified because it is the cleaved, active form of α-ENaC (14, 15). To demonstrate that Nedd8 has a role in the proteolytic degradation of ENaC, we performed a cycloheximide chase assay using isolated alveolar T2 cells with and without MLN4924 (Fig. 4*E*). Inhibition of Nedd8 with MLN4924 significantly attenuated ENaC degradation at 60 and 120 min ($n = 3$, * = $p < 0.05$). Corresponding patch clamp data shown in Fig. 5 (obtained from alveolar T1 cells) and Fig. 6 (obtained from alveolar T2 cells) show that MLN4924 significantly increases HSC channel and NSC channel activity in both alveolar epithelial cell types. In particular, ENaC NPo increased from 0.34 ± 0.20 to 0.82 ± 0.30 (in T1 cells) and 0.07 ± 0.03 to 0.80 ± 0.16 (in T2 cells) ~1 h post-MLN4924 treatment. Collectively, these data demonstrate that Cullin-dependent ubiquitination of ENaC is redox-sensitive, as inhibiting activated Cullin (Nedd8 conjugated with Cullin-1) using H_2O_2 significantly increased ENaC protein expression and ENaC activity. Additionally, inhibition of activated Cullin using the Nedd8 E1 activating enzyme inhibitor, MLN4924 compound, attenuated ENaC protein degradation.

To verify that changes in single channel activity lead to altered lung function, we compared the effects of tracheally instilling C57Bl/6 mice with either 10 μM MLN4924 (Fig. 7, ●), 10 μM MLN4924 + 1 mM amiloride (○), or saline only (■). Consistent with our report that MLN4924 significantly increases ENaC HSC and NSC channel activity in alveolar cells, Fig. 7 shows that mouse lung instilled with 10 μM MLN4924 ($n = 7$) cleared the saline challenge at a rate significantly greater than saline control (saline only, $n = 15$) between 65–120 min

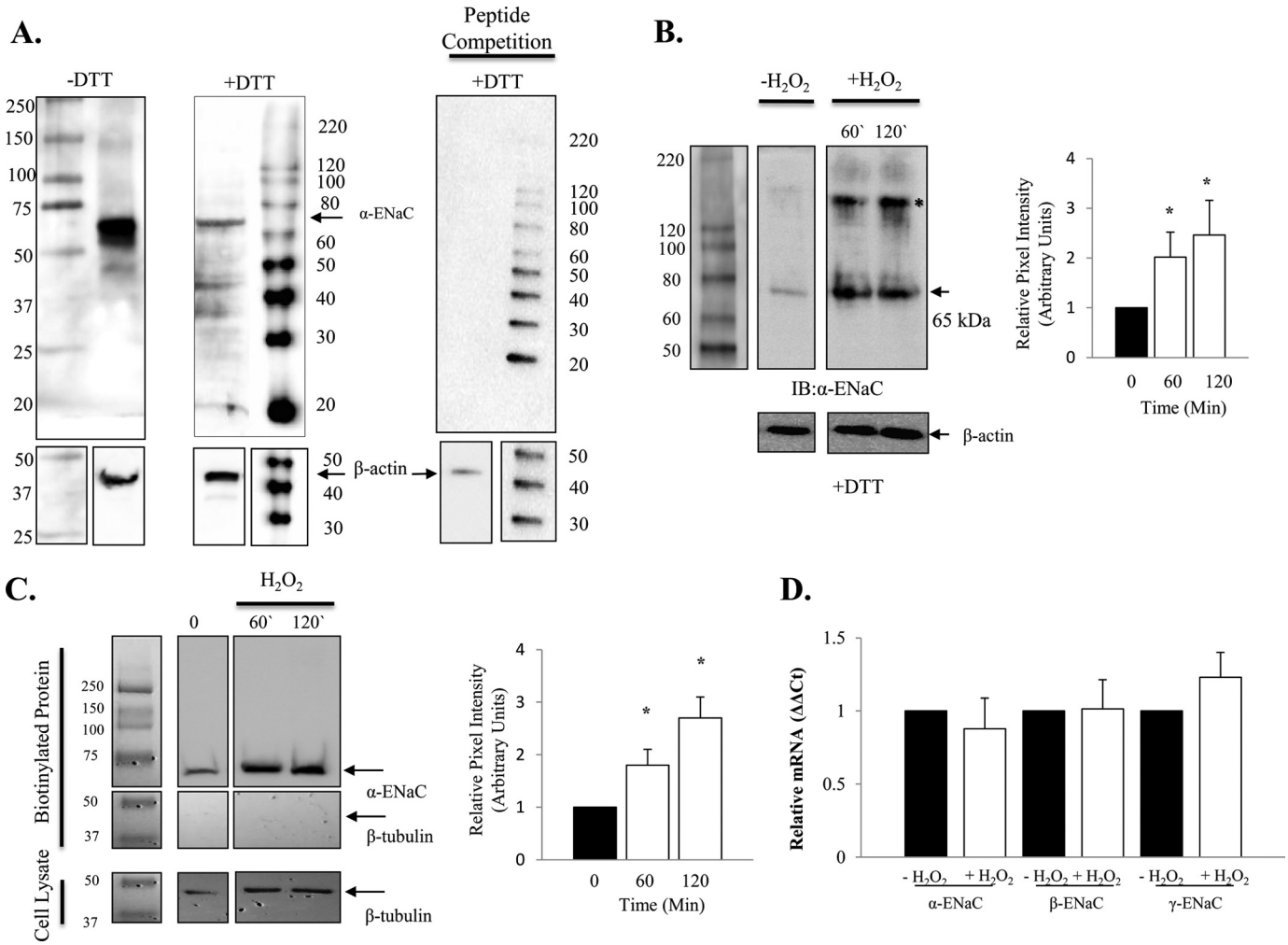

FIGURE 3. **H_2O_2 increases cell surface expression of α-ENaC in alveolar epithelial cells.** *A*, characterization of anti-α-ENaC C20 antibody under non-reducing (*-DTT*) and reducing (*+DTT*) conditions with a peptide competition assay (*right panel*) indicating antibody specificity and β-actin loading controls. *B*, representative blot and quantification of the 65-kDa α-ENaC immunoreactive band assayed from whole cell lysate following 0.5 mM H_2O_2 treatment. A larger, ~150-kDa band was also detected following hydrogen peroxide treatment and noted with an *asterisk*. *C*, representative blot and quantification of surface α-ENaC assayed from biotinylated T2 cells following treatment with 0.5 mM H_2O_2. *D*, 0.5 mM H_2O_2 did not affect relative ENaC subunit mRNA expression levels. $n = 3$. *, $p < 0.05$.

(as indicated with an *asterisk*). Importantly, coinstilling animals with MLN4924 and amiloride (○, $n = 10$) significantly attenuated the rate of lung fluid clearance at all time points compared with MLN4924-instilled animals (and between 0–60 min when compared with saline control animals, indicated by #). We also compared mice receiving MLN4924 with amiloride (○) to amiloride alone (□, $n = 15$) and did not detect a significant difference. Together, the data strongly indicate that the neddylation pathway plays an important role in regulating ENaC activity and, hence, lung fluid balance *in vivo*.

Redox Regulation of Nedd8 Ubiquitination of ENaC—Recent work by the Neish laboratory (16, 17) established that reactive oxygen species mediate changes in Cullin-1 and Nedd8 conjugation. Specifically, their research showed that reactive oxygen species cause oxidative inactivation of the catalytic cysteine residue of Ubc12, the Nedd8-conjugating enzyme. The resulting transient loss of Cullin-1 neddylation indeed altered cell signaling (17). To determine whether Nedd8 plays a role in proteolytic degradation of ENaC, we coimmunoprecipitated Cullin-1 and Nedd8 in the presence and absence of H_2O_2 and blotted for α-ENaC using an antibody directed against the C-terminal domain of α-ENaC. Fig. 8*A* shows decreased Cullin-1 and Nedd8 association with α-ENaC subunit under oxidizing conditions *(+ DTT)*, thus supporting the notion that the redox-sensitive Nedd8 signaling pathway regulates ENaC activity. The *right panel* in Fig. 8*A* provides a negative signal control for the immunoprecipitation studies performed, in which there was no α-ENaC detected following pull-down with IgG beads only. We also coimmunoprecipitated Ubc12, an ~20-kDa E2 enzyme, Fig. 8*C*, *left panel*) with α-ENaC subunit in the presence and absence of H_2O_2. H_2O_2 reduced ENaC and Ubc12 association. This ~85-kDa band is highlighted in Fig. 8*B* ($n = 3$, $p = 0.05$). Collectively, these data demonstrate that the formation of the Cullin-RING complex with ENaC is redox-sensitive.

Next we examined total protein ubiquitination in T2 cell extract (Fig. 8*C*), as well as the extent of α-ENaC polyubiquitination (*D*) from immunoprecipitated samples with and without exposure to H_2O_2. In Fig. 8*C*, we show that the level of ubiquitination in T2 cells is decreased significantly after 2 h of 0.5 mM H_2O_2 treatment ($n = 3$, $p = 0.01$, data normalized to β-actin

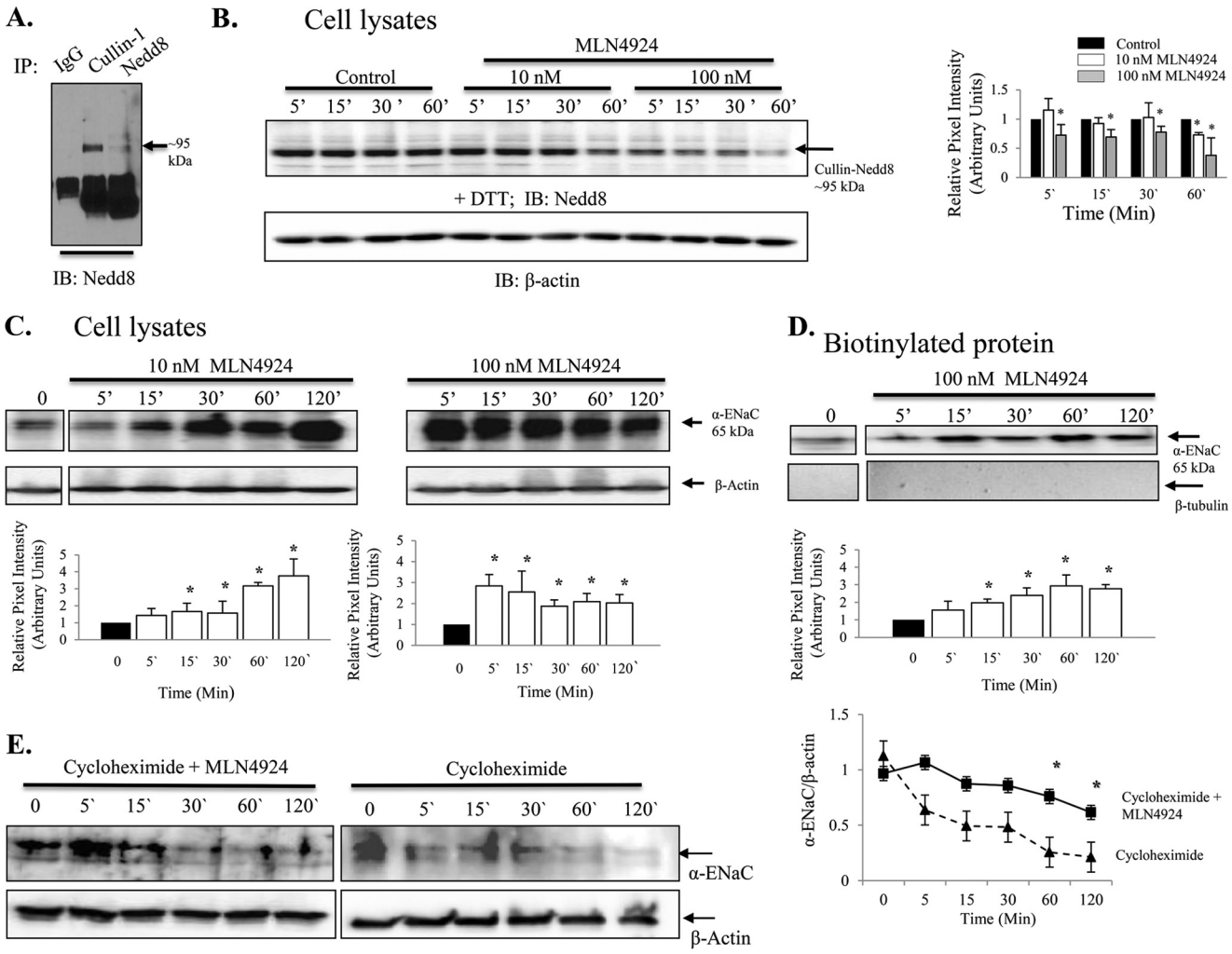

FIGURE 4. **MLN4924 decreases Nedd8 conjugation to Cullin-1 and increases the expression of α-ENaC in isolated rat alveolar T2 cells.** *A*, Western blot analysis (*IB*) demonstrating that in the presence of DTT the Cullin-1- Nedd8 conjugate is ~95 kDa. *IP*, immunoprecipitation. *B*, Western blot analysis depicting changes in Cullin1-Nedd8 conjugates in response to 10 nM and 100 nM MLN4924 with quantification of blots shown in a *bar graph*. *C*, Western blot analysis demonstrating an increase in total α-ENaC following treatment with 10 nM or 100 nM MLN4924. The *graphs* below show quantification of α-ENaC. *D*, Western blot analysis and *bar graph* demonstrating biotinylated α-ENaC expression following treatment with 100 nM MLN4924. *E*, a cycloheximide chase experiment shows preservation of α-ENaC expression in isolated rat T2 cells. $n = 3$. *, $p < 0.05$.

levels). To determine whether H_2O_2 specifically attenuates ENaC polyubiquitination, we immunoprecipitated α-ENaC from T2 cells in the presence or absence of 10 μM H_2O_2 and immunoblotted using P4D1 ubiquitin antibody (Cell Signaling Technology, Inc.). In Fig. 8*D*, *left panel*, we show α-ENaC antibody specificity in whole cell lysate. Quantification of the smear (signal between 220 – 65 kDa in each lane) indicates that H_2O_2 decreased ubiquitination of ENaC by ~40% ($p = 0.003$, $n = 4$).

DISCUSSION

Our laboratory has reported previously that glucocorticoids and mineralocorticoids, the principal steroid hormone regulators of ENaC, stimulate production of reactive oxygen species in sodium transporting epithelia (18). This finding indicates that steroid-hormone-receptor activation of ENaC may, in part, occur via regulated ROS signaling. In support of this, our laboratory has shown recently that sequestering superoxides with a superoxide mimetic, tetramethyl-piperidine oxide (TEMPO) and inhibition of NADPH oxidase (a superoxide-generating enzyme) with a Rac1-inhibiting compound similarly resulted in attenuation of normal ENaC activity (19). Conversely, application of exogenous superoxides using hypoxanthine and xanthine oxidase to cell-attached patch clamp recordings lead to substantial increases in ENaC activity (18), thereby enhancing net Na^+ transport. In this study, we report a plausible new mechanism by which ROS could be up-regulating sodium channel activity in the lung by attenuating proteolytic degradation of ENaC.

In Fig. 2, we show that moderately strong oxidizing agents such as hydrogen peroxide increase surface expression of ENaC in lung epithelial cells. Exposure of isolated primary alveolar T2 cells to hydrogen peroxide resulted in a time- and concentration-dependent increase in α-ENaC subunit expression, as determined by Western blot analysis and surface biotinylation assays. In our biochemical detection of ENaC, H_2O_2 increases the expression of the cleaved form of α-ENaC subunit (a 65-kDa band). In the literature, anti-α-ENaC antibody has been reported to immunoreact with both protein bands of apparent

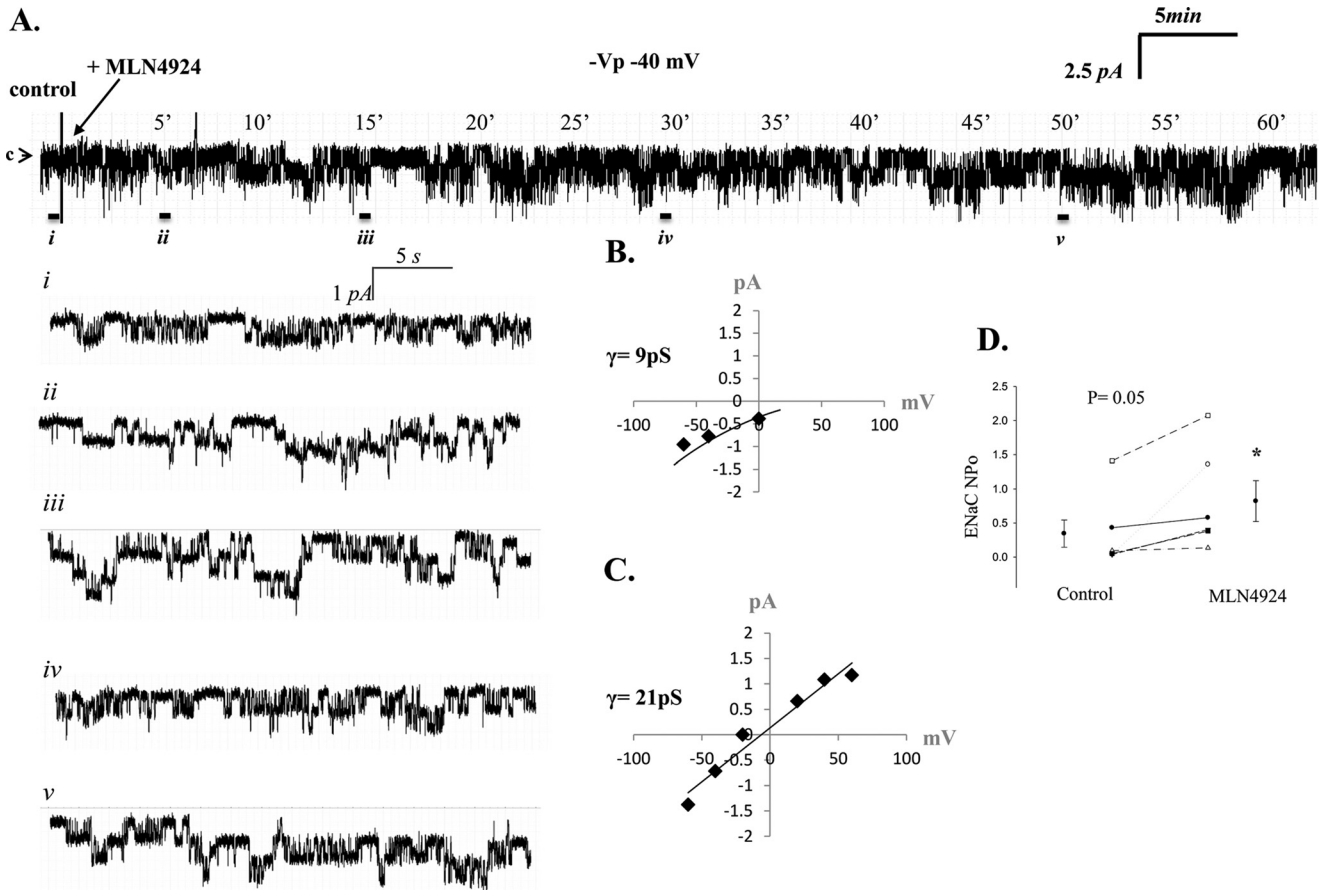

FIGURE 5. **MLN4924 increases ENaC activity in lung primary T1 cells.** *A*, representative single channel patch recording of a primary T1 cell in the cell-attached configuration. The *arrow* denotes the closed state, and *downward deflections* represent Na channel openings. Enlarged *insets* of the recording from the control (*i*) period and near 5 (*ii*), 15 (*iii*), 30 (*iv*) and 50 (*v*) min (*-40 mV, -Vp*) are shown. *B* and *C*, calculated chord conductance of HSC and NSC channels present in T1 cells. *D*, results from five independent observations shown on dot-plot graphs with *y* axis = ENaC activity (*NPo*) measured as the product of the number of channels (*N*) and the open probability (*Po*). *NPo* values increased from 0.34 ± 0.20 to 0.82 ± 0.30. $p = 0.05$.

masses near 85 kDa and 60 kDa in rat kidney epithelia (20), *Xenopus* A6 distal nephron cells (21), and lung epithelia (22). Using the same commercially available α-ENaC C-terminal C20 antibody (purchased from Santa Cruz Biotechnology, Inc.), our research group, alongside published reports by Dr. Baines' laboratory (23, 24), consistently detect the cleaved protein of ~65 kDa in human H441 airway or in rat epithelia, as reported here (Fig. 3). In a previous study, Xu and Chu (22) report the effects of hydrogen peroxide on α-ENaC protein expression, with the focus placed primarily on the declined detection of the 85-kDa band, in which the authors presumed to be an α2-ENaC variant following 24 h of 0.5 mM H_2O_2 treatment. Our study differs from this effect in that we report marked increases in surface expression of (cleaved ~65 kDa) α-ENaC following 4 h of 0.5 mM H_2O_2 treatment with no change in the ENaC subunit transcript (Fig. 3*C*). In contrast, the O'Brodovich laboratory (25) has shown that superoxide scavenger TEMPO decreases α-ENaC mRNA levels in fetal distal lung epithelial cells. These data, combined with our recent observations, suggest that reactive oxygen species can work through disparate signal transduction pathways to reinforce net salt and water reabsorption in the airways. ENaC mRNA expression is clearly associated with redox-sensitive NF-κβ transcription factor activation (for a review, see Ref. 26). In future studies, we propose to examine the effect of H_20_2 on each of the sodium channel subunit that comprises the architecture of ENaC 27–29.

Importantly, however, our studies also revealed that a larger (~150-kDa) band is immunoreactive using the C-20 anti-α-ENaC antibody following H_2O_2 treatment under reducing conditions (Fig. 3*B*). Although the molecular identity of this band is presently unknown, it is interesting to note the specificity of antibody used (Fig. 3*A*) and the conditions in which this larger band is detected. Because the gel presented in Fig. 3*B* is indeed reducing (+*DTT*), the larger band must represent non-covalent changes in α-ENaC protein following H_2O_2 exposure. Beyond the scope of this study, as a future area of the research interest of our laboratory we posit that the larger molecular weight band detected following H_2O_2 treatment could represent α-ENaC subunits with significant thiol modifications withstanding the effects of DTT.

Extensive studies in the past decade have revealed that surface expression of ENaC is tightly regulated by ubiquitin-mediated trafficking of surface-expressed ENaC (1, 12, 30–33). Ubiquitination of ENaC by the Nedd4-2 ubiquitin ligase (a HECT domain-containing E3 ligase) has been shown to affect post-trafficking and degradation of ENaC via the lysosomal or the proteasomal pathways (20, 21). In this study, we examined post-translational modification of ENaC activity by redox-sen-

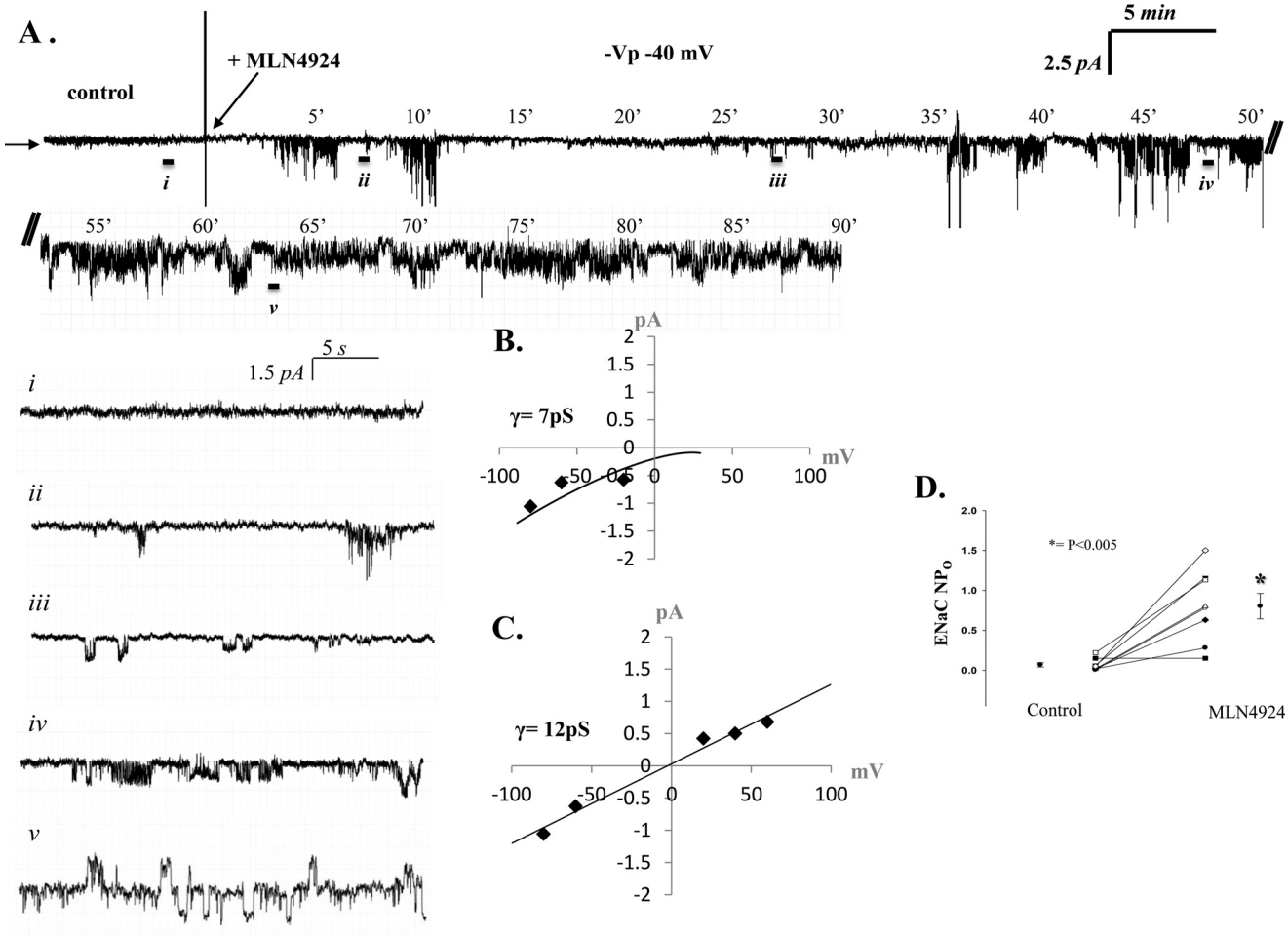

FIGURE 6. **MLN4924 increases ENaC activity in isolated rat alveolar T2 cells.** A, representative single channel patch recording of alveolar T2 cell in the cell-attached configuration. The *arrow* denotes the closed state, and *downward deflections* represent Na^+ channel openings and breaks in the recording (indicated with //). Again, enlarged excerpts of the control (*i*) period recording and at ~7.5 (*ii*), 27.5 (*iii*), 47.5 (*iv*) and 62.5 (*v*) min (*-40 mV* (*-Vp*)) are shown. *B* and *C*, IV curves depicting the calculated chord conductance of HSC channels (*7pS*) and NSC (*12pS*) channels present in T2 cells. *D*, results from eight independent observations shown on dot-plot graphs with *y* axis = ENaC activity (*NPo*), where *n* = number of channels and Po = open probability. *NPo* values increased from 0.07 ± 0.03 to 0.80 ± 0.16. $p < 0.005$.

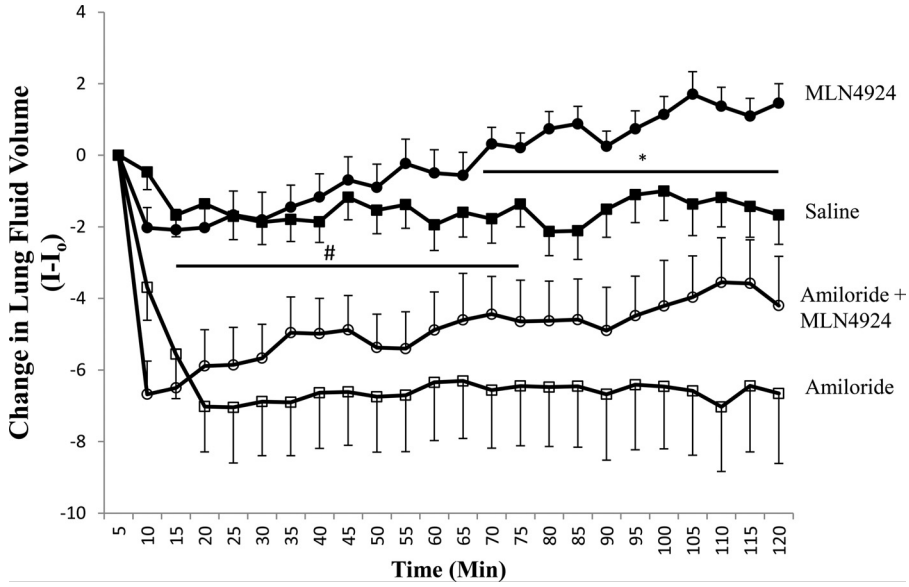

FIGURE 7. **MLN4924 increases lung clearance *in vivo*.** *Line graph* showing changes in lung fluid clearance presented with time on the *x* axis and I-I_o on the *y* axis, where *I* is the x-ray density at a respective time and I_o is the initial x-ray density following the tracheal instillation. Mice received a tracheal instillation of either 10 μM MLN4924 (●), saline only (■), 10 μM MLN4924 with 1 mM amiloride (○), or 1 mM amiloride alone (□). *, $p < 0.01$; #, $p < 0.05$.

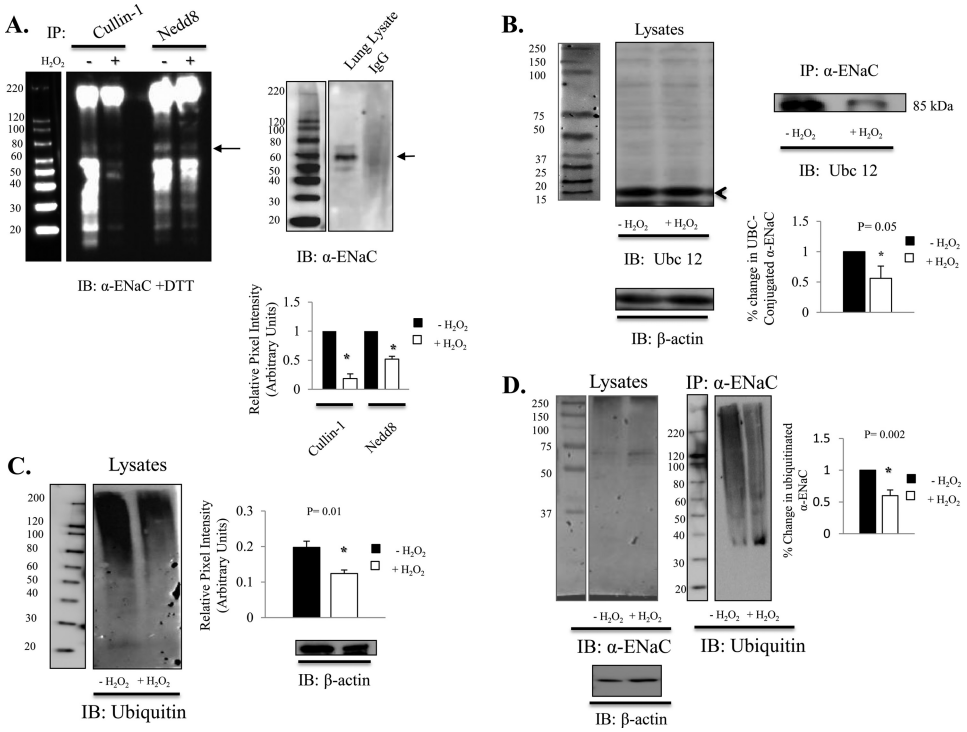

FIGURE 8. **Nedd8-mediated ubiquitination of α-ENaC is redox-sensitive.** *A*, coimmunoprecipitation (*IP*) of Cullin-1 and Nedd8 with α-ENaC shown under denaturing (+*DTT*) conditions. The intense bands below 60 kDa are immunoglobulins. *IB*, immunoblot. *B*, coimmunoprecipitation of α-ENaC and Ubc12 from isolated T2 cell treated ± 0.5 mM H_2O_2. The *left panel* shows the predicted molecular weight for Ubc12. The *right panel* shows that H_2O_2 reduced Ubc 12 conjugated α-ENaC. $n = 3$. $p < 0.05$. *C*, T2 cell lysate was treated ± 0.5 mM H_2O_2 for 1 h, and the ubiquitinated protein was quantified using P4D1 ubiquitin antibody. Data were normalized to the β-actin expression level. $n = 3$. $p = 0.01$. *D*, α-ENaC was detected in T2 cell lysate (*left panel*). Ubiquitinated α-ENaC was detected (*right panel*) following immunoprecipitation of α-ENaC (using anti-α -ENaC C20 antibody and P4D1 ubiquitin antibody) in samples ± 2 h exposure to 0.5 mM H_2O_2. Quantification of immunoprecipitated α-ENaC (± 0.5 mM H_2O_2 exposure for 2 h) demonstrates an ~40% reduction in ubiquitination. $n = 4$. $p = 0.02$.

sitive pathways, such as neddylation. Nedd8 is a ubiquitin-like protein that can indeed regulate the number of active channels residing in the apical membrane. Previous studies by the Neish laboratory (13, 34) indicate that hydrogen peroxide controls neddylation of Cullin-1 and, hence, formation of a functional E3-ubiquitin ligase. On the basis of our results, we propose that in alveolar epithelial cells, ROS interferes with Nedd8 conjugation with Cullin-1, which would of course attenuate ubiquitination of lung ENaC. Further, we propose that ENaC is indeed a target of the neddylation pathway, as inhibition of Nedd8 activating enzyme significantly increases channel activity and clearance. Additionally, in Fig. 8, we show that α-ENaC is intimately associated with Cullin-1, Nedd8, and Ubc12. We focused primarily on evaluating α-ENaC subunit association with the E3-SCF complex as an initial first step in studying this novel mode of ENaC regulation, given that α-ENaC subunits (alone) can form functional channels (35, 36) and that, because of the three homologous subunits, loss of α-ENaC expression in the lung leads to a non-viable lung phenotype (32, 37).

This study puts forth a novel mechanism of redox-sensitive regulation of ENaC, indicating that inactivation of the neddylation pathway may be a useful point of intervention in pulmonary disorders such as acute lung injury and pulmonary edema. Interestingly, the Wei laboratory (35, 36) has shown recently that phosphorylation of Rictor at Thr-1135 impairs the Rictor·Cullin-1 complex (and no other Cullin family member) to ubiquitinate the serum and glucocorticoid kinase 1 (SGK1). Because SGK1 clearly interacts with the WW domains of Nedd4-2 (37–43), the important implication from the study of Wei *et al.* (35, 36) is that Cullin-1 can alter ENaC activity in a redox-sensitive manner (via neddylation) or via a non-ROS-dependent pathway (such as promoting SGK1 degradation after association with the Ricotor-mTOR complex). Normal and misdirected redox-sensitive pathways leading to altered sodium transport in lung epithelia is the focus of future studies.

REFERENCES

1. Firsov, D., Gautschi, I., Merillat, A. M., Rossier, B. C., and Schild, L. (1998) The heterotetrameric architecture of the epithelial sodium channel (ENaC). *EMBO J.* **17,** 344–352
2. Kelly, O., Lin, C., Ramkumar, M., Saxena, N. C., Kleyman, T. R., and Eaton, D. C. (2003) Characterization of an amiloride binding region in the α-subunit of ENaC. *Am. J. Physiol. Renal Physiol.* **285,** F1279–F1290
3. Hummler, E., and Rossier, B. C. (1996) Physiological and pathophysiological role of the epithelial sodium channel in the control of blood pressure. *Kidney Blood Press. Res.* **19,** 160–165
4. Staub, O., Gautschi, I., Ishikawa, T., Breitschopf, K., Ciechanover, A., Schild, L., and Rotin, D. (1997) Regulation of stability and function of the epithelial Na+ channel (ENaC) by ubiquitination. *EMBO J.* **16,** 6325–6336
5. Yu, L., Helms, M. N., Yue, Q., and Eaton, D. C. (2008) Single-channel analysis of functional epithelial sodium channel (ENaC) stability at the apical membrane of A6 distal kidney cells. *Am. J. Physiol. Renal Physiol.* **295,** F1519–F1527
6. Lazrak, A., Jurkuvenaite, A., Chen, L., Keeling, K. M., Collawn, J. F., Bedwell, D. M., and Matalon, S. (2011) Enhancement of alveolar epithelial sodium channel activity with decreased cystic fibrosis transmembrane

conductance regulator expression in mouse lung. *Am. J. Physiol. Lung Cell Mol. Physiol.* **301,** L557–L567
7. Lazrak, A., Chen, L., Jurkuvenaite, A., Doran, S. F., Liu, G., Li, Q., Lancaster, J. R., Jr., and Matalon, S. (2012) Regulation of alveolar epithelial Na+ channels by ERK1/2 in chlorine-breathing mice. *Am. J. Respir. Cell Mol. Biol.* **46,** 342–354
8. Staub, O., and Rotin, D. (1997) Regulation of ion transport by protein-protein interaction domains. *Curr. Opin. Nephrol. Hypertens.* **6,** 447–454
9. Kamitani, T., Kito, K., Nguyen, H. P., and Yeh, E. T. (1997) Characterization of NEDD8, a developmentally down-regulated ubiquitin-like protein. *J. Biol. Chem.* **272,** 28557–28562
10. Kumar, A., Wu, H., Collier-Hyams, L. S., Kwon, Y. M., Hanson, J. M., and Neish, A. S. (2009) The bacterial fermentation product butyrate influences epithelial signaling via reactive oxygen species-mediated changes in cullin-1 neddylation. *J. Immunol.* **182,** 538–546
11. Helms, M. N., Jain, L., Self, J. L., and Eaton, D. C. (2008) Redox regulation of epithelial sodium channels examined in alveolar type 1 and 2 cells patch-clamped in lung slice tissue. *J. Biol. Chem.* **283,** 22875–22883
12. Soucy, T. A., Smith, P. G., Milhollen, M. A., Berger, A. J., Gavin, J. M., Adhikari, S., Brownell, J. E., Burke, K. E., Cardin, D. P., Critchley, S., Cullis, C. A., Doucette, A., Garnsey, J. J., Gaulin, J. L., Gershman, R. E., Lublinsky, A. R., McDonald, A., Mizutani, H., Narayanan, U., Olhava, E. J., Peluso, S., Rezaei, M., Sintchak, M. D., Talreja, T., Thomas, M. P., Traore, T., Vyskocil, S., Weatherhead, G. S., Yu, J., Zhang, J., Dick, L. R., Claiborne, C. F., Rolfe, M., Bolen, J. B., and Langston, S. P. (2009) An inhibitor of NEDD8-activating enzyme as a new approach to treat cancer. *Nature* **458,** 732–736
13. Goodson, P., Kumar, A., Jain, L., Kundu, K., Murthy, N., Koval, M., and Helms, M. N. (2012) NADPH oxidase regulates alveolar epithelial sodium channel activity and lung fluid balance *in vivo* via O^- signaling. *Am. J. Physiol. Lung Cell Mol. Physiol.* **302,** L410–L419
14. Kleyman, T. R., Carattino, M. D., and Hughey, R. P., (2009) ENaC at the cutting edge. Regulation of epithelial sodium channels by proteases. *J. Biol. Chem.* **284,** 20447–20451
15. Rossier, B. C., and Stutts, M. J., (2009) Activation of the epithelial sodium channel (ENaC) by serine proteases. *Annu. Rev. Physiol.* **71,** 361–379
16. Kumar, A., Collier-Hyams, L., Kwon, Y. M., Hanson, J. M., and Neish, A. S. (2011) Buyrate influences epithelial signaling via generation of reactive oxygen species. *FASEB J.* **22,** 328
17. Kumar, A., Wu, H., Collier-Hyams, L. S., Hansen, J. M., Li, T., Yamoah, K., Pan, Z. Q., Jones, D. P., and Neish, A. S. (2007) Commensal bacteria modulate cullin-dependent signaling via generation of reactive oxygen species. *EMBO J.* **26,** 4457–4466
18. Yu, L., Bao, H. F., Self, J. L., Eaton, D. C., and Helms, M. N. (2007) Aldosterone-induced increases in superoxide production counters nitric oxide inhibition of epithelial Na channel activity in A6 distal nephron cells. *Am. J. Physiol. Renal Physiol.* **293,** F1666–F1677
19. Takemura, Y., Goodson, P., Bao, H. F., Jain, L., and Helms, M. N. (2010) Rac1-mediated NADPH oxidase release of O_2- regulates epithelial sodium channel activity in the alveolar epithelium. *Am. J. Physiol. Lung Cell Mol. Physiol.* **298,** L509–L520
20. Ergonul, Z., Frindt, G., and Palmer, L. G. (2006) Regulation of maturation and processing of ENaC subunits in the rat kidney. *Am. J. Physiol. Renal Physiol.* **291,** F683–F693
21. Alvarez de la Rosa, D., Li, H., and Canessa, C. M. (2002) Effects of aldosterone on biosynthesis, traffic, and functional expression of epithelial sodium channels in A6 cells. *J. Gen. Physiol.* **119,** 427–442
22. Xu, H., and Chu, S. (2007) ENaC alpha-subunit variants are expressed in lung epithelial cells and are suppressed by oxidative stress. *Am. J. Physiol. Lung Cell Mol. Physiol.* **293,** L1454–L1462
23. Baines, D. L., Albert, A. P., Hazell, M. J., Gambling, L., Woollhead, A. M., and Dockrell, M. E. (2010) Lipopolysaccharide modifies amiloride-sensitive Na+ transport processes across human airway cells. Role of mitogen-activated protein kinases ERK 1/2 and 5. *Pflugers Arch.* **459,** 451–463
24. Tan, C. D., Selvanathar, I. A., and Baines, D. L. (2011) Cleavage of endogenous γENaC and elevated abundance of αENaC are associated with increased Na(+) transport in response to apical fluid volume expansion in human H441 airway epithelial cells. *Pflugers Arch.* **462,** 431–441
25. Rafii, B., Tanswell, A. K., Otulakowski, G., Pitkänen, O., Belcastro-Taylor, R., and O'Brodovich, H. (1998) O_2-induced ENaC expression is associated with NF-κB activation and blocked by superoxide scavenger. *Am. J. Physiol.* **275**: L764–L770
26. Flohé, L., Brigelius-Flohé, R., Saliou, C., Traber, M. G., and Packer, L. (1997) Redox regulation of NF-κ B activation. *Free Radic. Biol. Med.* **22,** 1115–1126
27. Ismailov, I. I., Awayda, M. S., Berdiev, B. K., Bubien, J. K., Lucas, J. E., Fuller, C. M., and Benos, D. J. (1996) Triple-barrel organization of ENaC, a cloned epithelial Na+ channel. *J. Biol. Chem.* **271,** 807–816
28. Stewart, A. P., Haerteis, S., Diakov, A., Korbmacher, C., and Edwardson, J. M. (2011) Atomic force microscopy reveals the architecture of the epithelial sodium channel (ENaC). *J. Biol. Chem.* **286,** 31944–31952
29. Stockand, J. D., Staruschenko, A., Pochynyuk, O., Booth, R. E., and Silverthorn, D. U. (2008) Insight toward epithelial Na+ channel mechanism revealed by the acid-sensing ion channel 1 structure. *IUBMB Life* **60,** 620–628
30. Kabra, R., Knight, K. K., Zhou, R., and Snyder, P. M. (2008) Nedd4-2 induces endocytosis and degradation of proteolytically cleaved epithelial Na+ channels. *J. Biol. Chem.* **283,** 6033–6039
31. Kamynina, E., and Staub, O. (2002) Concerted action of ENaC, Nedd4-2, and Sgk1 in transepithelial Na(+) transport. *Am. J. Physiol. Renal Physiol.* **283,** F377–F387
32. Snyder, P. M., Steines, J. C., and Olson, D. R. (2004) Relative contribution of Nedd4 and Nedd4-2 to ENaC regulation in epithelia determined by RNA interference. *J. Biol. Chem.* **279,** 5042–5046
33. Zhou, R., Patel, S. V., and Snyder, P. M. (2007) Nedd4-2 catalyzes ubiquitination and degradation of cell surface ENaC. *J. Biol. Chem.* **282,** 20207–20212
34. Helms, M. N., Torres-Gonzalez, E., Goodson, P., and Rojas, M. (2010) Direct tracheal instillation of solutes into mouse lung. *J. Vis. Exp.* **42,** 1941
35. Gao, D., Wan, L., Inuzuka, H., Berg, A. H., Tseng, A., Zhai, B., Shaik, S., Bennett, E., Tron, A. E., Gasser, J. A., Lau, A., Gygi, S. P., Harper, J. W., DeCaprio, J. A., Toker, A., and Wei, W. (2010) Rictor forms a complex with Cullin-1 to promote SGK1 ubiquitination and destruction. *Mol. Cell* **39,** 797–808
36. Gao, D., Wan, L., and Wei, W. (2010) Phosphorylation of Rictor at Thr-1135 impairs the Rictor/Cullin-1 complex to ubiquitinate SGK1. *Protein Cell* **1,** 881–885
37. Snyder, P. M., Olson, D. R., Kabra, R., Zhou, R., and Steines, J. C. (2004) cAMP and serum and glucocorticoid-inducible kinase (SGK) regulate the epithelial Na(+) channel through convergent phosphorylation of Nedd4-2. *J. Biol. Chem.* **279,** 45753–45758
38. Asher, C., Sinha, I., and Garty, H. (2003) Characterization of the interactions between Nedd4-2, ENaC, and sgk-1 using surface plasmon resonance. *Biochim. Biophys. Acta* **1612,** 59–64
39. Boehmer, C., Palmada, M., Rajamanickam, J., Schniepp, R., Amara, S., and Lang, F. (2006) Post-translational regulation of EAAT2 function by co-expressed ubiquitin ligase Nedd4-2 is impacted by SGK kinases. *J. Neurochem.* **97,** 911–921
40. Li, T., Koshy, S., and Folkesson, H. G. (2009) IL-1β-induced cortisol stimulates lung fluid absorption in fetal guinea pigs via SGK-mediated Nedd4-2 inhibition. *Am. J. Physiol. Lung Cell Mol. Physiol.* **296,** L527–L533
41. Pearce, D. (2003) SGK1 regulation of epithelial sodium transport. *Cell Physiol. Biochem.* **13,** 13–20
42. Snyder, P. M., Olson, D. R., and Thomas, B. C. (2002) Serum and glucocorticoid-regulated kinase modulates Nedd4-2-mediated inhibition of the epithelial Na+ channel. *J. Biol. Chem.* **277,** 5–8
43. Wiemuth, D., Lott, J. S., Ly, K., Ke, Y., Teesdale-Spittle, P., Snyder, P. M., and McDonald, F. J. (2010) Interaction of serum- and glucocorticoid regulated kinase 1 (SGK1) with the WW-domains of Nedd4-2 is required for epithelial sodium channel regulation. *PLoS ONE* **5,** e12163